

# We are IntechOpen, the world's leading publisher of Open Access books Built by scientists, for scientists

6,900

Open access books available

185,000

International authors and editors

200M

Downloads

Our authors are among the

154

Countries delivered to

TOP 1%

most cited scientists

12.2%

Contributors from top 500 universities



WEB OF SCIENCE™

Selection of our books indexed in the Book Citation Index  
in Web of Science™ Core Collection (BKCI)

Interested in publishing with us?  
Contact [book.department@intechopen.com](mailto:book.department@intechopen.com)

Numbers displayed above are based on latest data collected.  
For more information visit [www.intechopen.com](http://www.intechopen.com)



# Boundary Element Model for Nonlinear Fractional-Order Heat Transfer in Magneto-Thermoelastic FGA Structures Involving Three Temperatures

*Mohamed Abdelsabour Fahmy*

## Abstract

The principal objective of this chapter is to introduce a new fractional-order theory for functionally graded anisotropic (FGA) structures. This theory called nonlinear uncoupled magneto-thermoelasticity theory involving three temperatures. Because of strong nonlinearity, it is very difficult to solve the problems related to this theory analytically. Therefore, it is necessary to develop new numerical methods for solving such problems. So, we propose a new boundary element model for the solution of general and complex problems associated with this theory. The numerical results are presented graphically in order to display the effect of the graded parameter on the temperatures and displacements. The numerical results also confirm the validity and accuracy of our proposed model.

**Keywords:** boundary element method, fractional-order heat transfer, functionally graded anisotropic structures, nonlinear uncoupled magneto-thermoelasticity, three temperatures

## 1. Introduction

Functionally graded material (FGM) is a special type of advanced inhomogeneous materials. Functionally graded structure is a mixture of two or more distinct materials (usually heat-resisting ceramic on the outside surface and fracture-resisting metal on the inside surface) that have specified properties in specified direction of the structure to achieve a require function [1, 2]. This feature enables obtaining structures with the best of both material's properties, and suitable for applications requiring high thermal resistance and high mechanical strength [3–12].

Functionally Graded Materials have been wide range of thermoelastic applications in several fields, for example, the water-cooling model of a fusion reactor divertor is one of the most widely used models in industrial design, which is consisting of a tungsten (W) and a copper (Cu), that subjected to a structural integrity issue due to thermal stresses resulted from thermal expansion mismatch between the bond materials. Recently, functionally graded tungsten (W)–copper (Cu) has been developed by using a precipitation-hardened copper alloy as matrix

instead of pure copper, to overcome the loss of strength due to the softening of the copper matrix.

The carbon nanotubes (CNT) in FGM have new applications such as reinforced functionally graded piezoelectric actuators, reinforced functionally graded polyester calcium phosphate materials for bone replacement, reinforced functionally graded tools and dies for reduce scrap, better wear resistance, better thermal management, and improved process productivity, reinforced metal matrix functionally graded composites used in mining, geothermal drilling, cutting tools, drills and machining of wear resistant materials. Also, they used as furnace liners and thermal shielding elements in microelectronics.

There are many areas of application for elastic and thermoelastic functionally graded materials, for example, industrial applications such as MRI scanner cryogenic tubes, eyeglass frames, musical instruments, pressure vessels, fuel tanks, cutting tool inserts, laptop cases, wind turbine blades, firefighting air bottles, drilling motor shaft, X-ray tables, helmets and aircraft structures. Automobiles applications such as combustion chambers, engine cylinder liners, leaf springs, diesel engine pistons, shock absorbers, flywheels, drive shafts and racing car brakes. Aerospace applications rocket nozzle, heat exchange panels, spacecraft truss structure, reflectors, solar panels, camera housing, turbine wheels and Space shuttle. Submarine applications such as propulsion shaft, cylindrical pressure hull, sonar domes, diving cylinders and composite piping system. Biotechnology applications such as functional gradient nanohydroxyapatite reinforced polyvinyl alcohol gel biocomposites. Defense applications such as armor plates and bullet-proof vests. High-temperature environment applications such as aerospace and space vehicles. Biomedical applications such as orthopedic applications for teeth and bone replacement. Energy applications such as energy conversion devices and as thermoelectric converter for energy conservation. They also provide thermal barrier and are used as protective coating on turbine blades in gas turbine engine. Marine applications such as parallelogram slabs in buildings and bridges, swept wings of aircrafts and ship hulls. Optoelectronic applications such as automobile engine components, cutting tool insert coating, nuclear reactor components, turbine blade, tribology, sensors, heat exchanger, fire retardant doors, etc.

According to continuous and smooth variation of FGM properties throughout in depth, there are many laws to describe the behavior of FGM such as index [13], sigmoid law [14], exponential law [15] and power law [16–24].

There was widespread interest in functionally graded materials, which has developed a lot of analytical methods for analysis of elasticity [25–32] and thermoelasticity [33–53] problems, some of which have become dominant in scientific literature. For the numerical methods, the isogeometric finite element method (FEM) has been used by Valizadeh et al. [54] for static characteristics of FGM and by Bhardwaj et al. [55] for solving crack problem of FGM. Nowadays, the boundary element method is a simple, efficient and powerful numerical tool which provides an excellent alternative to the finite element method for the solution of FGM problems, Sladek et al. [56–58] have been developed BEM formulation for transient thermal problems in FGMs. Gao et al. [59] developed fracture analysis of functionally graded materials by a BEM. Fahmy [60–72] developed BEM to solve elastic, thermoelastic and biomechanic problems in anisotropic functionally graded structures. Further details on the BEM are given in [73, 74] and the references therein.

In the present paper, we propose new FGA structures theory and new boundary element technique for modeling problems of nonlinear uncoupled magneto-thermoelasticity involving three temperatures. The boundary element method reduces the dimension of the problem, therefore, we obtain a reduction of numerical approximation, linear equations system and input data. Since there is strong nonlinearity in the proposed theory and its related problems. So, we develop new

boundary element technique for modeling such problems. The numerical results are presented graphically through the thickness of the homogeneous and functionally graded structures to show the effect of graded parameter on the temperatures and displacements. The numerical results demonstrate the validity and accuracy of our proposed model.

A brief summary of the chapter is as follows: Section 1 outlines the background and provides the readers with the necessary information to books and articles for a better understanding of mechanical behaviour of magneto-thermoelastic FGA structures and their applications. Section 2 describes the formulation of the new theory and its related problems. Section 3 discusses the implementation of the new BEM for solving the nonlinear radiative heat conduction equation, to obtain the three temperature fields. Section 4 studies the development of new BEM and its implementation for solving the move equation based on the known three temperature fields, to obtain the displacement field. Section 5 presents the new numerical results that describe the through-thickness mechanical behaviour of homogeneous and functionally graded structures.

## 2. Formulation of the problem

We consider a Cartesian coordinate system for 2D structure (see **Figure 1**) which is functionally graded along the 0x direction, and considering z-axis is the direction of the effect of the constant magnetic field  $H_0$ .

The fractional-order governing equations of three temperatures nonlinear uncoupled magneto-thermoelasticity in FGA structures can be written as follows [6].

$$\sigma_{pj,j} + \tau_{pj,j} = \rho(x+1)^m \ddot{u}_k \quad (1)$$

$$\sigma_{pj} = (x+1)^m [C_{pjkl} u_{k,l} - \beta_{pj} T_\alpha(r, \tau)] \quad (2)$$

$$\tau_{pj} = \mu(x+1)^m (h_p H_j + H_j h_p - \delta_{pj} (h_k H_k)) \quad (3)$$

where  $\sigma_{pj}, \tau_{pj}, u_k, C_{pjkl}$  ( $C_{pjkl} = C_{klpj} = C_{kljp}$ ),  $\beta_{pj}$  ( $\beta_{pj} = \beta_{jp}$ ),  $\mu$  and  $h_p$  are respectively, mechanic stress tensor, Maxwell stress tensor, displacement, constant elastic moduli, stress-temperature coefficients, magnetic permeability and perturbed magnetic field.

The nonlinear time-dependent two dimensions three temperature (2D-3 T) radiation diffusion equations coupled by electron, ion and phonon temperatures may be written as follows

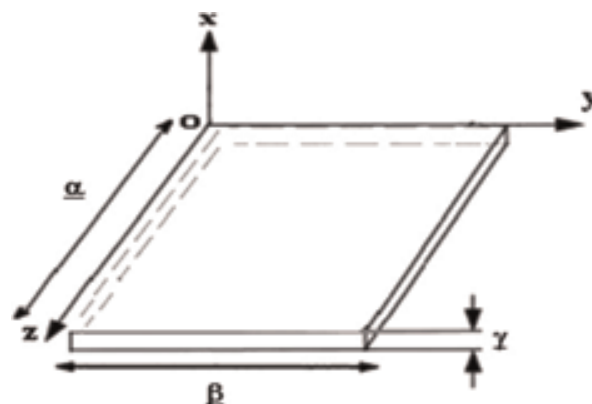


**Figure 1.**  
 Geometry of the FGA structure.

$$D_\tau^\alpha T_\alpha(r, \tau) = \xi \nabla [\mathbb{K}_\alpha \nabla T_\alpha(r, \tau)] + \xi \bar{\mathbb{W}}(r, \tau), \xi = \frac{1}{c_\alpha \rho \delta_1} \quad (4)$$

where

$$\bar{\mathbb{W}}(x, y, \tau) = \begin{cases} -\rho \mathbb{W}_{ei} (T_e - T_i) - \rho \mathbb{W}_{er} (T_e - T_r), & \alpha = e, \delta_1 = 1 \\ \rho \mathbb{W}_{ei} (T_e - T_i), & \alpha = i, \delta_1 = 1 \\ \rho \mathbb{W}_{ep} (T_e - T_p), & \alpha = p, \delta_1 = \frac{4}{\rho} T_p^3 \end{cases} \quad (5)$$

and

$$\mathbb{W}_{ei} = \rho \mathbb{A}_{ei} T_e^{-2/3}, \mathbb{W}_{ep} = \rho \mathbb{A}_{ep} T_e^{-1/2} \mathbb{K}_\alpha = \mathbb{A}_\alpha T_\alpha^{5/2}, \alpha = e, i, \mathbb{K}_p = \mathbb{A}_p T_p^{3+\mathbb{B}} \quad (6)$$

The total energy per unit mass can be expressed as follows

$$P = P_e + P_i + P_p, P_e = c_e T_e, P_i = c_i T_i, P_p = \frac{1}{\rho} c_p T_p^4 \quad (7)$$

where  $\mathbb{K}_\alpha$  are conductive coefficients,  $T_\alpha$  are temperature functions,  $c_\alpha$  ( $\alpha = e, i, p$ ) are isochore specific-heat coefficients,  $\rho$  is the density,  $\tau$  is the time. In which,  $c_\alpha$ ,  $\mathbb{A}_\alpha$  ( $\alpha = e, i, p$ ),  $\mathbb{B}$ ,  $\mathbb{A}_{ei}$ ,  $\mathbb{A}_{ep}$  are constant inside each subdomain,  $\mathbb{W}_{ei}$  and  $\mathbb{W}_{ep}$  are electron-ion coefficient and electron-phonon coefficient, respectively.

Initial and boundary conditions can be written as

$$T_\alpha(r, 0) = T_\alpha^0(r) = g_1(r, \tau), \quad (8)$$

$$u_k(r, 0) = \dot{u}_k(r, 0) = 0 \text{ for } r \in R \cup C(r, \tau), \quad (9)$$

$$\mathbb{K}_\alpha \frac{\partial T_\alpha}{\partial n} \Big|_{\Gamma_1} = 0, \alpha = e, i, T_r|_{\Gamma_1} = g_2(r, \tau) \quad (10)$$

$$u_k(r, \tau) = \Psi_k(r, \tau) \text{ for } r \in C_3 \quad (11)$$

$$t_k(r, \tau) = \delta_k(r, \tau) \text{ for } r \in C_4, C = C_3 \cup C_4, C_3 \cap C_4 = \emptyset \quad (12)$$

$$\mathbb{K}_\alpha \frac{\partial T_\alpha}{\partial n} \Big|_{\Gamma_2} = 0, \alpha = e, i, p \quad (13)$$

$$T(r, \tau) = H(r, \tau) \text{ for } r \in C_1, \quad \tau > 0 \quad (14)$$

$$q(r, \tau) = h(r, \tau) \text{ for } r \in C_2, \quad \tau > 0, C = C_1 \cup C_2, C_1 \cap C_2 = \emptyset \quad (15)$$

### 3. BEM numerical implementation for temperature field

This section outlines the solution of 2D nonlinear time-dependent three temperatures (electron, ion and phonon) radiation diffusion equations using a boundary element method.

Now, let us consider  $\xi = \frac{1}{c_\alpha \rho \delta_1} = 1$  and discretize the time interval  $[0, F]$  into  $F + 1$  equal time steps, where  $\tau^f = f \Delta \tau, f = 0, 1, 2, \dots, F$ . Let  $T^f(\mathbf{x}) = T(\mathbf{x}, \tau^f)$  be the solution at time  $\tau^f$ . Assuming that the time derivative of temperature within the time interval  $[\tau^f, \tau^{f+1}]$  can be approximated by.

$$\dot{T}_\alpha(r, \tau) = \frac{T_\alpha^{f+1}(r) - T_\alpha^f(r)}{\Delta \tau} + O(\Delta \tau) \quad (16)$$

$D_\tau^a$  denotes the Caputo fractional time derivative of order  $a$  defined by [75].

$$D_\tau^a T_\alpha(r, \tau) = \frac{1}{\Gamma(1-a)} \int_0^\tau \frac{\partial T_\alpha(r, s)}{\partial s} \frac{ds}{(\tau-s)^a}, 0 < a < 1 \quad (17)$$

By using a finite difference scheme of Caputo fractional time derivative of order  $a$  (17) at times  $(f + 1)\Delta \tau$  and  $f\Delta \tau$ , we obtain:

$$D_\tau^a T_\alpha^{f+1} + D_\tau^a T_\alpha^f \approx \sum_{j=0}^k W_{a,j} (T_\alpha^{f+1-j}(r) - T_\alpha^{f-j}(r)), (f = 1, 2, \dots, F) \quad (18)$$

Where

$$W_{a,0} = \frac{(\Delta \tau)^{-a}}{\Gamma(2-a)} \quad (19)$$

$$W_{a,j} = W_{a,0} ((j+1)^{1-a} - (j-1)^{1-a}), j = 1, 2, \dots, F \quad (20)$$

According to Eq. (18), the fractional order heat Eq. (4) can be replaced by the following system

$$\begin{aligned} & W_{a,0} T_\alpha^{f+1}(r) - \mathbb{K}_\alpha(x) T_{\alpha,II}^{f+1}(r) - \mathbb{K}_{\alpha,I}(x) T_{\alpha,I}^{f+1}(r) \\ & = W_{a,0} T_\alpha^f(r) - \mathbb{K}_\alpha(x) T_{\alpha,II}^f(r) - \mathbb{K}_{\alpha,I}(x) T_{\alpha,I}^f(r) \\ & - \sum_{j=1}^f W_{a,j} (T_\alpha^{f+1-j}(r) - T_\alpha^{f-j}(r)) + \overline{\mathbb{W}}_m^{f+1}(x, \tau) + \overline{\mathbb{W}}_m^f(x, \tau), f = 0, 1, 2, \dots, F \end{aligned} \quad (21)$$

According to Fahmy [60], and using the fundamental solution which satisfies the system (21), the boundary integral equations corresponding to nonlinear three temperature heat conduction-radiation equations can be written as

$$CT_\alpha = \frac{D}{\mathbb{K}_\alpha} \int_0^\tau \int_S [T_\alpha q^* - T_\alpha^* q] dS d\tau + \frac{D}{\mathbb{K}_\alpha} \int_0^\tau \int_R b T_\alpha^* dR d\tau + \int_R T_\alpha^i T_\alpha^*|_{\tau=0} dR \quad (22)$$

which can be written in the absence of internal heat sources as follows

$$CT_\alpha = \int_S [T_\alpha q^* - T_\alpha^* q] dS - \int_R \frac{\mathbb{K}_\alpha}{D} \frac{\partial T_\alpha^*}{\partial \tau} T_\alpha dR \quad (23)$$

Time temperature derivative can be written as

$$\frac{\partial T_\alpha}{\partial \tau} \cong \sum_{j=1}^N f^j(r)^j a^j(\tau) \quad (24)$$

where  $f^j(r)$  are known functions and  $a^j(\tau)$  are unknown coefficients.

We suppose that  $\hat{T}_\alpha^j$  is a solution of

$$\nabla^2 \hat{T}_\alpha^j = f^j \quad (25)$$

Then, Eq. (23) yields the following boundary integral equation

$$CT = \int_S [T_\alpha q^* - T_\alpha^* q] dS + \sum_{j=1}^N a^j(\tau) D^{-1} \left( C \hat{T}_\alpha^j - \int_S [T_\alpha^j q^* - \hat{q}^j T_\alpha^*] dS \right) \quad (26)$$

where

$$\hat{q}^j = -\mathbb{K}_\alpha \frac{\partial \hat{T}_\alpha^j}{\partial n} \quad (27)$$

and

$$a^j(\tau) = \sum_{i=1}^N f_{ji}^{-1} \frac{\partial T(r_i, \tau)}{\partial \tau} \quad (28)$$

In which the entries of  $f_{ji}^{-1}$  are the coefficients of  $F^{-1}$  with matrix  $F$  defined as [76].

$$\{F\}_{ii} = f^j(r_i) \quad (29)$$

Using the standard boundary element discretization scheme for Eq. (26) and using Eq. (28), we have

$$C \dot{T}_\alpha + H T_\alpha = G Q \quad (30)$$

The diffusion matrix can be defined as

$$C = -[H \hat{T}_\alpha - G \hat{Q}] F^{-1} D^{-1} \quad (31)$$

with

$$\{\hat{T}\}_{ij} = \hat{T}^j(\mathbf{x}_i) \quad (32)$$

$$\{\hat{Q}\}_{ij} = \hat{q}^j(\mathbf{x}_i) \quad (33)$$

In order to solve Eq. (30) numerically the functions  $T_\alpha$  and  $q$  are interpolated as

$$T_\alpha = (1 - \theta) T_\alpha^m + \theta T_\alpha^{m+1} \quad (34)$$

$$q = (1 - \theta) q^m + \theta q^{m+1} \quad (35)$$

where  $\theta = \frac{\tau - \tau^m}{\tau^{m+1} - \tau^m}$ ,  $0 \leq \theta \leq 1$  determines the practical time  $\tau$  in the current time step.

By differentiating Eq. (34) with respect to time we get

$$\dot{T}_\alpha = \frac{dT_\alpha}{d\theta} \frac{d\theta}{d\tau} = \frac{T_\alpha^{m+1} - T_\alpha^m}{\tau^{m+1} - \tau^m} = \frac{T_\alpha^{m+1} - T_\alpha^m}{\Delta\tau^m} \quad (36)$$

The substitution of Eqs. (34)–(36) into Eq. (30) leads to

$$\left(\frac{C}{\Delta\tau^m} + \theta H\right) T_\alpha^{m+1} - \theta G Q^{m+1} = \left(\frac{C}{\Delta\tau^m} - (1 - \theta)H\right) T_\alpha^m + (1 - \theta)G Q^m \quad (37)$$

By using initial and boundary conditions, we get

$$\mathbf{aX} = \mathbf{b} \quad (38)$$

This system yields the temperature, that can be used to solve (1) for the displacement.

#### 4. BEM numerical implementation for displacement field

Based on Eqs. (2) and (3), Eq. (1) can be rewritten as

$$L_{jl}u_k = \rho\ddot{u}_p - (D_{jl}u_k + D_{pj}T_\alpha) = \rho\ddot{u}_p - \rho b_p = \rho b'_p \quad (39)$$

where

$$L_{jl} = D_l \frac{\partial}{\partial x_j}, D_{jl} = \mu H_0^2 D_j \frac{\partial}{\partial x_l}, D_{pj} = -\beta_{pj} D_j, D_l = C_{pjkl} \frac{\partial}{\partial x_l}, D_j = \left(\frac{\partial}{\partial x_j} + \Lambda\right), \Lambda = \frac{m}{x+1} \quad (40)$$

when the temperatures are known, the displacement can be computed by solving (39) using BEM. By choosing  $u_p^*$  as the weight function and applying the weighted residual method, Eq. (39) can be reexpressed as

$$\int_{\mathbf{R}} (L_{jl}u_k - \rho b_p')u_p^* d\mathbf{R} = 0 \quad (41)$$

The first term in (41) can be integrated partially using Gau  $\beta$  theory yields

$$\int_{\mathbf{R}} C_{pjkl}u_{k,lj}u_p^* d\mathbf{R} = \int_{\mathbf{C}} C_{pjkl}u_{k,l}u_p^* n_j d\mathbf{C} - \int_{\mathbf{R}} C_{pjkl}u_{k,l}u_{p,j}^* d\mathbf{R} \quad (42)$$

The last term in (42) can be integrated partially twice using Gau  $\beta$  theory yields

$$\int_{\mathbf{R}} C_{pjkl}u_{k,l}u_{p,j}^* d\mathbf{R} = \int_{\mathbf{C}} C_{pjkl}u_{k,l}u_{p,j}^* n_l d\mathbf{C} - \int_{\mathbf{R}} C_{pjkl}u_{k,l}u_{p,jl}^* d\mathbf{R} \quad (43)$$

Based on Eq. (43), Eq. (42) can be rewritten as

$$\int_{\mathbf{R}} C_{pjkl}u_{k,lj}u_p^* d\mathbf{R} - \int_{\mathbf{R}} C_{pjkl}u_{k,l}u_{p,jl}^* d\mathbf{R} = \int_{\mathbf{C}} C_{pjkl}u_{k,l}u_p^* n_j d\mathbf{C} - \int_{\mathbf{C}} C_{pjkl}u_{k,l}u_{p,j}^* n_l d\mathbf{C} \quad (44)$$

which can be written as

$$\int_{\mathbf{R}} (L_{jl}u_k \cdot u_p^* - L_{jl}^*u_k^* \cdot u_p) d\mathbf{R} = \int_{\mathbf{C}} (G_{jl}u_k \cdot u_p^* - G_{jl}^*u_k^* \cdot u_p) d\mathbf{C} \quad (45)$$

The boundary tractions are

$$t_p = C_{pjkl}u_{k,l}n_j = G_{jl}u_k \text{ and } t_p^* = C_{pjkl}u_{k,j}^*n_l = G_{jl}^*u_k^* \quad (46)$$

By using the symmetry relation of elasticity tensor, we obtain

$$L_{jl} = C_{pjkl} \mathfrak{N} \frac{\partial^2}{\partial x_l \partial x_j} = C_{kjpil} \mathfrak{N} \frac{\partial^2}{\partial x_j \partial x_l} = L_{jl}^* \quad (47)$$

$$G_{jl} = C_{pjkl} \mathfrak{N} n_j \frac{\partial}{\partial x_l} = C_{kjpil} \mathfrak{N} n_l \frac{\partial}{\partial x_j} = G_{jl}^* \quad (48)$$

Using Eqs. (46)–(48), the Eq. (45) can be reexpressed as

$$\int_{\mathbf{R}} (C_{pjkl}u_{k,lj} \cdot u_p^* - C_{pjkl}u_{k,lj}^* \cdot u_p) d\mathbf{R} = \int_{\mathbf{C}} (t_p u_p^* - t_p^* u_p) d\mathbf{C} \quad (49)$$

We define the fundamental solution  $u_{mk}^*$  by the relation

$$L_{jl}u_{mk}^* = -\delta(x, \xi)\delta_{pm} \quad (50)$$

By modifying the weighting functions, Eq. (49) can be written as

$$\int_{\mathbf{R}} (C_{pjkl}u_{k,lj} \cdot u_{mp}^* - C_{pjkl}u_{mk,lj}^* \cdot u_p) d\mathbf{R} = \int_{\mathbf{C}} (t_p u_{mp}^* - t_{mp}^* u_p) d\mathbf{C} \quad (51)$$

From (39), (50) and (51), the representation formula may be written as

$$u_m(\xi) = \int_C (u_{mp}^*(x, \xi) t_p(x) - t_{mp}^*(x, \xi) u_p(x)) dC - \int_R u_{mp}^*(x, \xi) \rho b_p'(x) dR \quad (52)$$

Let

$$\begin{aligned} \rho b_p' &= -((D_{jl} + D_{pk} + \Lambda D_l) u_k + D_{pj} T_\alpha) \\ &\approx \sum_{q=1}^N f_{pn}^q \alpha_n^q = \sum_{q=1}^N (L_{jl} u_{kn}^q) \alpha_n^q, D_{pk} = -\rho \delta_{pk} \frac{\partial^2}{\partial \tau^2} \end{aligned} \quad (53)$$

The displacement particular solution may be defined as

$$u_{kn}^q = \delta_{kn} (r^2 + r^3) \quad (54)$$

Differentiation of (54) leads to.

$$u_{kn,l}^q = \delta_{kn} (2r + 3r^2) r_{,l}, \quad u_{kn,li}^q = \delta_{kn} ((2 + 3r) \delta_{li} + 3rr_{,j} r_{,l}) \quad (55)$$

Now, we obtain the traction particular solution  $t_{pn}^q$  and source function  $f_{pn}^q$  as

$$t_{pn}^q = C_{pjkl} u_{kn,l}^q n_j, \quad L_{jl} u_{kn}^q = f_{pn}^q \quad (56)$$

The domain integral may be approximated as follows

$$\int_R u_{mp}^* \rho b_p' dR \approx \sum_{q=1}^N \left( \int_R (L_{jl} u_{kn}^q u_{mp}^*) dR \right) \alpha_n^q \quad (57)$$

The use of (57) together with the dual reciprocity

$$\int_R (L_{jl} u_{kn}^q u_{mp}^* - L_{jl} u_{mk}^* u_{pn}^q) dR = \int_C (u_{mp}^* t_{pn}^q - t_{mp}^* u_{pn}^q) dC \quad (58)$$

Leads to

$$\begin{aligned} \int_R u_{mp}^* \rho b_p' dR &= \sum_{q=1}^N \int_R (L_{jl} u_{mk}^* u_{pn}^q) dR \\ &+ \int_C (u_{mp}^* t_{pn}^q - t_{mp}^* u_{pn}^q) dC \quad (59) \end{aligned}$$

From (50), we can write

$$\int_{\mathbf{R}} L_{jl} u_{mk}^* u_{pn}^q d\mathbf{R} = \int_{\mathbf{R}} -\delta(x, \xi) \delta_{pm} u_{pn}^q d\mathbf{R} = -u_{mn}^q(\xi) \quad (60)$$

By using (52), (59) and (60), we obtain

$$u_m(\xi) = \int_{\mathbf{C}} (u_{mp}^* t_p - t_{mp}^* u_p) d\mathbf{C} + \sum_{q=1}^N \left( u_{mn}^q(\xi) - \int_{\mathbf{C}} (u_{mp}^* t_{pn}^q - t_{mp}^* u_{pn}^q) d\mathbf{C} \right) \alpha_n^q \quad (61)$$

According to Fahmy [9–11], the right-hand side integrals of (61) can be reexpressed as

$$\begin{aligned} & \int_{\mathbf{C}} (u_{mp}^*(x, \xi) t_p(x) - t_{mp}^*(x, \xi) u_p(\xi)) d\mathbf{C} \\ &= \lim_{\varepsilon \rightarrow 0} \int_{\mathbf{C}-\mathbf{C}_\varepsilon} (u_{mp}^*(x, \xi) t_p(x) - t_{mp}^*(x, \xi) u_p(\xi)) d\mathbf{C} \\ &+ \lim_{\varepsilon \rightarrow 0} \int_{\mathbf{C}_\varepsilon} (u_{mp}^*(x, \xi) t_p(x) - t_{mp}^*(x, \xi) u_p(\xi)) d\mathbf{C}_\varepsilon \end{aligned} \quad (62)$$

and

$$\begin{aligned} & \int_{\mathbf{C}} (u_{mp}^*(x, \xi) t_{pn}^q(x) - t_{mp}^*(x, \xi) u_{pn}^q(\xi)) d\mathbf{C} = \\ & \lim_{\varepsilon \rightarrow 0} \int_{\mathbf{C}-\mathbf{C}_\varepsilon} (u_{mp}^*(x, \xi) t_{pn}^q(x) - t_{mp}^*(x, \xi) u_{pn}^q(\xi)) d\mathbf{C} \\ & + \lim_{\varepsilon \rightarrow 0} \int_{\mathbf{C}_\varepsilon} (u_{mp}^*(x, \xi) t_{pn}^q(x) - t_{mp}^*(x, \xi) u_{pn}^q(\xi)) d\mathbf{C}_\varepsilon \end{aligned} \quad (63)$$

According to Fahmy [12], Guiggiani and Gigante [77] and Mantič [78] Eqs. (62) and (63) can respectively be expressed as

$$\begin{aligned} & \int_{\mathbf{C}} (u_{mp}^*(x, \xi) t_p(x) - t_{mp}^*(x, \xi) u_p(\xi)) d\mathbf{C} \\ &= \int_{\mathbf{C}} u_{mp}^* t_p d\Gamma - \oint_{\mathbf{C}} u_p t_{mp}^* d\Gamma - c_{pj} u_p(\xi) \end{aligned} \quad (64)$$

$$\begin{aligned} & \int_{\mathbf{C}} (u_{mp}^*(x, \xi) t_{pn}^q(x) - t_{mp}^*(x, \xi) u_{pn}^q(\xi)) d\mathbf{C} \\ &= \int_{\mathbf{C}} u_{mp}^* t_{pn}^q d\Gamma - \oint_{\mathbf{C}} u_{pn}^q t_{mp}^* d\Gamma - c_{pj} u_{pn}^q(\varepsilon) \end{aligned} \quad (65)$$

By using (64) and (65), the dual reciprocity boundary integral equation becomes

$$c_{pj}u_p(\varepsilon) + \oint_C u_p t_{mp}^* d\Gamma - \int_C u_{mp}^* t_p d\Gamma = \sum_{q=1}^N \left( c_{pj}u_{pn}^q(\varepsilon) + \oint_C u_{pn}^q t_{mp}^* d\Gamma - \int_C u_{mp}^* t_{pn}^q d\Gamma \right) \alpha_n^q \quad (66)$$

On the basis of isoparametric concept, we can write

$$\{u, t\} \approx \sum_{k=1}^N \varphi_k \{\check{u}_k, \check{t}_k\} = \Phi^T \{\check{u}, \check{t}\} \quad (67)$$

$$\{u^q, t^q\} \approx \sum_{k=1}^N \varphi_k \{\check{u}_k^q, \check{t}_k^q\} = \Phi^T \{\check{u}^q, \check{t}^q\} \quad (68)$$

By implementing the point collocation procedure and using (67) and (68), Eq. (66) may be reexpressed as

$$\zeta \check{u} - \eta \check{t} = \sum_{q=1}^N (\zeta \check{u}^q - \eta \check{t}^q) \alpha^q(\tau) \quad (69)$$

Let us suppose that

$$\check{U} = [\check{u}^1 \ \check{u}^2 \ \dots \ \check{u}^N] \quad (70)$$

$$\check{\rho} = [\check{t}^1 \ \check{t}^2 \ \dots \ \check{t}^N] \quad (71)$$

$$\alpha = [\alpha^1 \ \alpha^2 \ \dots \ \alpha^N]^T \quad (72)$$

We can write (69) as follows

$$\zeta \check{u}(\tau) - \eta \check{t}(\tau) = (\zeta \check{U} - \eta \check{\rho}) \alpha(\tau) \quad (73)$$

By using the point collocation procedure,  $\alpha(\tau)$  can be calculated from (53) as

$$\rho \check{u}(\tau) - \rho \check{b}(\tau) = F \alpha(\tau) \quad (74)$$

Now, from (74), we may derive

$$\alpha(\tau) = F^{-1}(\rho \check{u}(\tau) - \rho \check{b}(\tau)) \quad (75)$$

From (73) using (75) we have

$$\mathcal{M} \check{u} + \zeta \check{u} = \eta \check{t}(\tau) + \check{B}(\tau) \quad (76)$$

where

$$\mathbf{U} = (\eta\check{\phi} - \zeta\check{U})F^{-1}, \quad \mathcal{M} = \rho\mathbf{U}, \quad \check{\mathcal{B}}(\tau) = \rho\mathbf{U}\check{b}(\tau). \quad (77)$$

By considering the following known  $k$  and unknown  $u$  superscripts nodal vectors

$$\{\check{u}^k, \check{t}^u\} \in C_3, \{\check{u}^u, \check{t}^k\} \in C_4 \quad (78)$$

Hence (76) may be written as

$$\begin{bmatrix} \mathcal{M}^{11} & \mathcal{M}^{12} \\ \mathcal{M}^{21} & \mathcal{M}^{22} \end{bmatrix} \begin{bmatrix} \check{u}^k(\tau) \\ \check{u}^u(\tau) \end{bmatrix} + \begin{bmatrix} \zeta^{11} & \zeta^{12} \\ \zeta^{21} & \zeta^{22} \end{bmatrix} \begin{bmatrix} \check{u}^k(\tau) \\ \check{u}^u(\tau) \end{bmatrix} = \begin{bmatrix} \eta^{11} & \eta^{12} \\ \eta^{21} & \eta^{22} \end{bmatrix} \begin{bmatrix} \check{t}^k(\tau) \\ \check{t}^u(\tau) \end{bmatrix} + \begin{bmatrix} \check{\mathcal{B}}^1(\tau) \\ \check{\mathcal{B}}^2(\tau) \end{bmatrix} \quad (79)$$

From the first row of (79), we can calculate the unknown fluxes  $\check{t}^u(\tau)$  as follows

$$\begin{aligned} \check{t}^u(\tau) &= (\eta^{12})^{-1} [\mathcal{M}^{11}\check{u}^k(\tau) + \mathcal{M}^{12}\check{u}^u(\tau) + \zeta^{11}\check{u}^k(\tau) \\ &+ \zeta^{12}\check{u}^u(\tau) - \eta^{11}\check{t}^k(\tau) - \check{\mathcal{B}}^1(\tau)] \end{aligned} \quad (80)$$

From the second row of (79) and using (80) we get

$$\mathcal{M}^u\check{u}^u(\tau) + \zeta^u\check{u}^u(\tau) = Q^k(\tau) \quad (81)$$

where

$$Q^k(\tau) = \check{\mathcal{B}}^k(\tau) + \eta^k\check{t}^k(\tau) - \mathcal{M}^k\check{u}^k(\tau) - \zeta^k\check{u}^k(\tau)$$

$$\mathcal{M}^u = \mathcal{M}^{22} - \eta^{22}(\eta^{12})^{-1}\mathcal{M}^{12}$$

$$\zeta^u = \zeta^{22} - \eta^{22}(\eta^{12})^{-1}\zeta^{12} \quad (82)$$

$$\mathcal{M}^k = \mathcal{M}^{21} - \eta^{22}(\eta^{12})^{-1}\mathcal{M}^{11}$$

$$\zeta^k = \zeta^{21} - \eta^{22}(\eta^{12})^{-1}\zeta^{11}$$

$$\check{\mathcal{B}}^k(\tau) = \mathcal{B}^2(\tau) - \eta^{22}(\eta^{12})^{-1}\mathcal{B}^1(\tau)$$

Eq. (81) can be written at  $(n + 1)$  time step as

$$\mathcal{M}^u\check{u}_{n+1}^u(\tau) + \zeta^u\check{u}_{n+1}^u(\tau) = Q_{n+1}^k(\tau) \quad (83)$$

where

$$Q_{n+1}^k(\tau) = \check{\mathcal{B}}_{n+1}^k(\tau) + \eta^k\check{t}_{n+1}^k(\tau) - \mathcal{M}^k\check{u}_{n+1}^k(\tau) - \zeta^k\check{u}_{n+1}^k(\tau) \quad (84)$$

In order to solve (83), The implicit backward finite difference scheme has been applied based on the Houbolt's algorithm and the following approximations

$$\check{u}_{n+1} \approx \frac{1}{6\Delta t} (11\check{u}_{n+1} - 18\check{u}_n + 9\check{u}_{n-1} - 2\check{u}_{n-2}) \quad (85)$$

$$\check{u}_{n+1} \approx \frac{1}{\Delta t^2} (2\check{u}_{n+1} - 5\check{u}_n + 4\check{u}_{n-1} - \check{u}_{n-2}) \quad (86)$$

By using (85) and (86), we have from (83)

$$\zeta^u \check{u}_{n+1}^u(\tau) = Q_{n+1}^k(\tau) \quad (87)$$

In which,

$$\zeta^u = \frac{2\mathcal{M}^u}{\Delta t^2} + \zeta^u \quad (88)$$

$$Q_{n+1}^k = Q_{n+1}^k + \frac{\mathcal{M}^u}{\Delta t^2} (5\check{u}_n - 4\check{u}_{n-1} + \check{u}_{n-2}) \quad (89)$$

We implement the successive over-relaxation (SOR) of Golub and Van Loan [79] for solving (87) to obtain  $\check{u}_{n+1}^u$ . Then, the unknown  $\check{u}_{n+1}^u$  and  $\check{u}_{n+1}^u$  can be obtained from (76) and (77), respectively. By using the procedure of Bathe [80], we obtain the traction vector  $t_{n+1}^u$  from (73).

## 5. Numerical results and discussion

The BEM that has been used in the current paper can be applicable to a wide variety of FGA structures problems associated with the proposed theory of three temperatures nonlinear uncoupled magneto-thermoelasticity. In order to evaluate the influence of graded parameter on the three temperatures and displacements, the numerical results are carried out and depicted graphically for homogeneous ( $m = 0$ ) and functionally graded ( $m = 0.5$  and  $1.0$ ) structures.

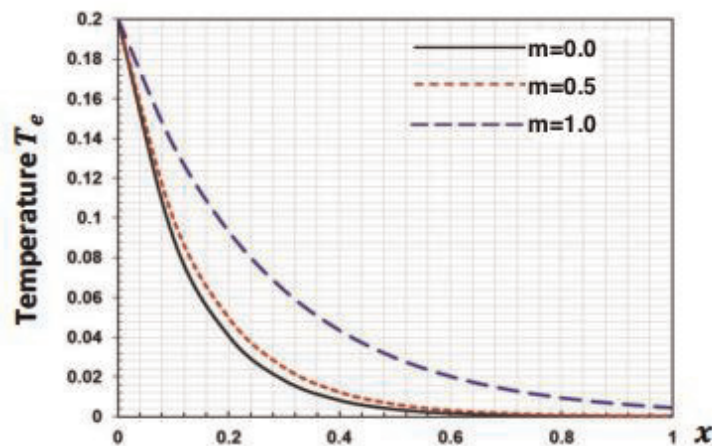


**Figure 2.**  
 Variation of the electron temperature  $T_e$  through the thickness coordinate  $x$ .

Figures 2–4 show the distributions of the three temperatures  $T_e$ ,  $T_i$  and  $T_p$  through the thickness coordinate  $Ox$ . It was shown from these figures that the three temperatures increase with increasing value of graded parameter  $m$ .

Figures 5 and 6 show the distributions of the displacements  $u_1$  and  $u_2$  through the thickness coordinate  $Ox$ . It was noticed from these figures that the displacement components increase with increasing value of graded parameter  $m$ .

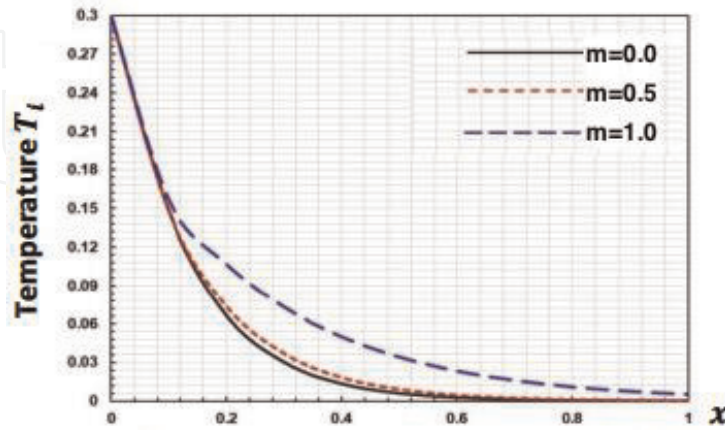


Figure 3.  
Variation of the ion temperature  $T_i$  through the thickness coordinate  $x$ .

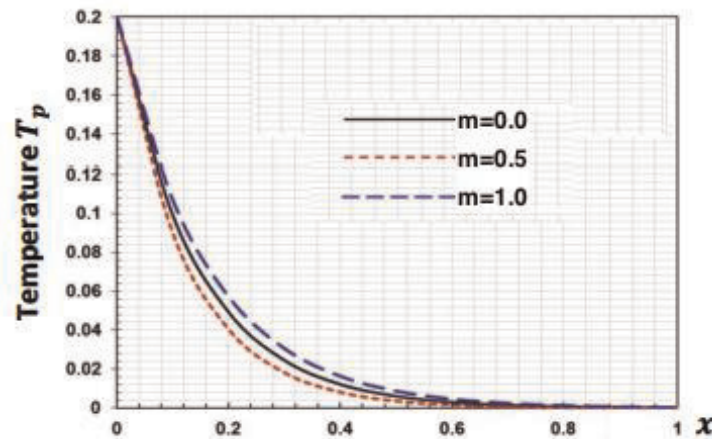


Figure 4.  
Variation of the photon temperature  $T_p$  through the thickness coordinate  $x$ .

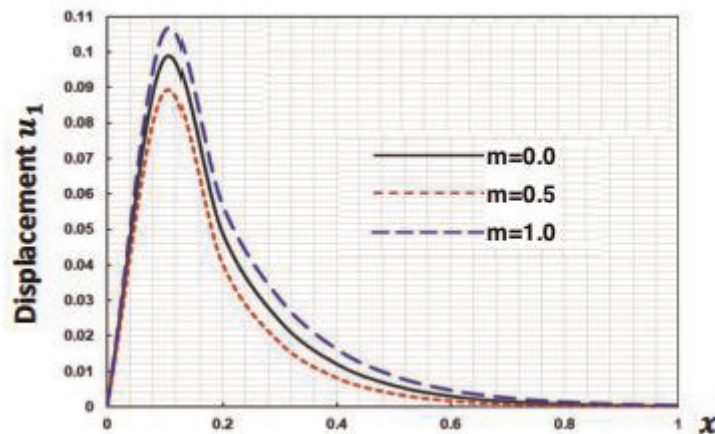


Figure 5.  
Variation of the displacement  $u_1$  through the thickness coordinate  $x$ .

Figures 7 and 8 show the distributions of the displacements  $u_1$  and  $u_2$  with the time for boundary element method (BEM), finite difference method (FDM) and finite element method (FEM) to demonstrate the validity and accuracy of our proposed technique. It is noted from numerical results that the BEM obtained results are agree quite well with those obtained using the FDM of Pazera and Jędrzyiak [81] and FEM of Xiong and Tian [82] results based on replacing heat conduction with three-temperature heat conduction.

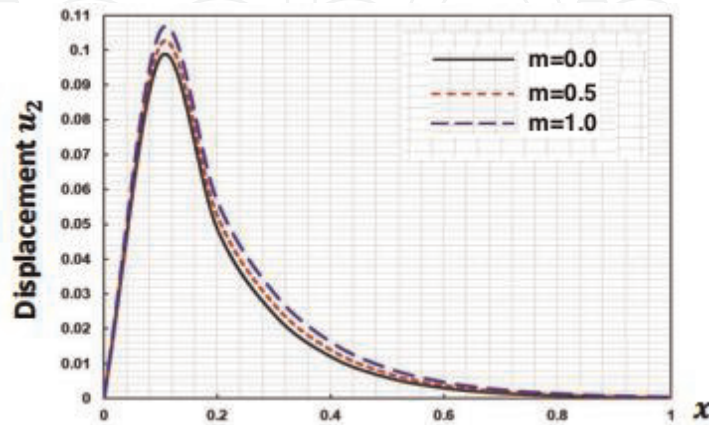


Figure 6.  
Variation of the displacement  $u_2$  through the thickness coordinate  $x$ .

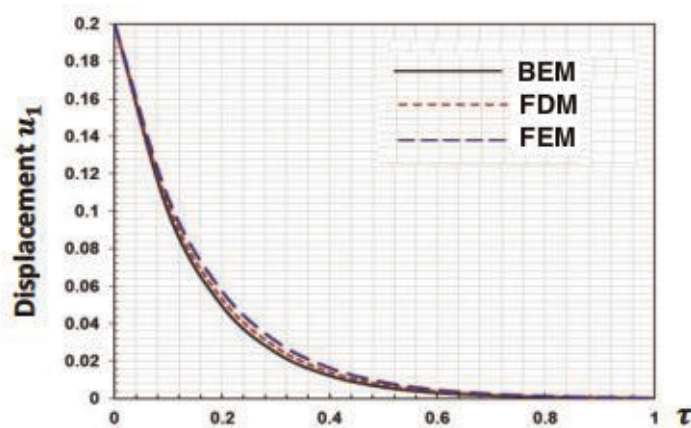


Figure 7.  
Variation of the displacement  $u_1$  with time  $\tau$ .

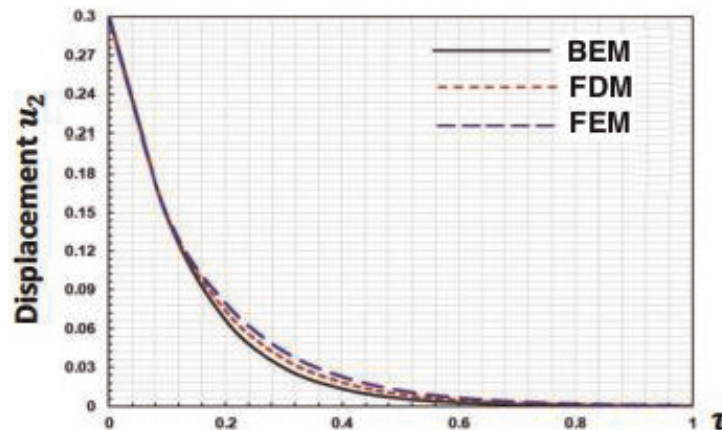


Figure 8.  
Variation of the displacement  $u_2$  with time  $\tau$ .

## 6. Conclusion

The main aim of this article is to introduce a new fractional-order theory called nonlinear uncoupled magneto-thermoelasticity theory involving three temperatures for FGA structures and new boundary element technique for solving problems related to the proposed theory. Since the nonlinear three temperatures radiative heat conduction equation is independent of the displacement field, we first determine the temperature field using the BEM, then based on the known temperature field, the displacement field is obtained by solving the move equation using the BEM. It can be seen from the numerical results that the graded parameter had a significant effect on the temperatures and displacements through the thickness of the functionally graded structures. Since there are no available results for the considered problem. So, some literatures may be considered as special cases from the considered problem based on replacing the heat conduction by three temperatures radiative heat conduction. The numerical results demonstrate the validity and accuracy of our proposed model. From the proposed BEM technique that has been performed in the present paper, it is possible to conclude that the proposed BEM should be applicable to any FGM uncoupled magneto-thermoelastic problem with three-temperature. BEM is more efficient, accurate and easy to use than FDM or FEM, because it only needs to solve the unknowns on the boundaries and BEM users need only to deal with real geometry boundaries. Also, BEM is reducing the computational cost of its solver. The present numerical results for our complex problem may provide interesting information for computer scientists, designers of new FGM materials and researchers in FGM science as well as for those working on the development of new functionally graded structures.

IntechOpen

### Author details

Mohamed Abdelsabour Fahmy

Faculty of Computers and Informatics, Suez Canal University, Ismailia, Egypt

\*Address all correspondence to: [mohamed\\_fahmy@ci.suez.edu.eg](mailto:mohamed_fahmy@ci.suez.edu.eg)

### IntechOpen

© 2019 The Author(s). Licensee IntechOpen. This chapter is distributed under the terms of the Creative Commons Attribution License (<http://creativecommons.org/licenses/by/3.0>), which permits unrestricted use, distribution, and reproduction in any medium, provided the original work is properly cited. 

## References

- [1] Reddy JN. Analysis of functionally graded plated. *International Journal for Numerical Methods in Engineering*. 2000;**47**:663-384
- [2] Reddy JN. *Mechanics of Laminated Composite Plates and Shells*. 2nd ed. Boca Raton, FL: CRC Press, LLC; 2004
- [3] Abd-Alla AM, Fahmy MA, El-Shahat TM. Magneto-thermo-elastic problem of a rotating non-homogeneous anisotropic solid cylinder. *Archive of Applied Mechanics*. 2008;**78**:135-148
- [4] Fahmy MA. Thermoelastic stresses in a rotating non-homogeneous anisotropic body. *Numerical Heat Transfer, Part A: Applications*. 2008;**53**: 1001-1011
- [5] Fahmy MA, El-Shahat TM. The effect of initial stress and inhomogeneity on the thermoelastic stresses in a rotating anisotropic solid. *Archive of Applied Mechanics*. 2008;**78**:431-442
- [6] Fahmy MA. A time-stepping DRBEM for magneto-thermo-viscoelastic interactions in a rotating nonhomogeneous anisotropic solid. *International Journal of Applied Mechanics*. 2011;**3**:1-24
- [7] El-Naggar AM, Abd-Alla AM, Fahmy MA, Ahmed SM. Thermal stresses in a rotating non-homogeneous orthotropic hollow cylinder. *Heat and Mass Transfer*. 2002;**39**:41-46
- [8] Abd-Alla AM, El-Naggar AM, Fahmy MA. Magneto-thermoelastic problem in non-homogeneous isotropic cylinder. *Heat and Mass Transfer*. 2003;**39**: 625-629
- [9] Fahmy MA. A time-stepping DRBEM for the transient magneto-thermo-viscoelastic stresses in a rotating non-homogeneous anisotropic solid. *Engineering Analysis with Boundary Elements*. 2012;**36**:335-345
- [10] Fahmy MA. Transient magneto-thermoviscoelastic plane waves in a non-homogeneous anisotropic thick strip subjected to a moving heat source. *Applied Mathematical Modelling*. 2012;**36**:4565-4578
- [11] Fahmy MA. The effect of rotation and inhomogeneity on the transient magneto-thermoviscoelastic stresses in an anisotropic solid. *ASME Journal of Applied Mechanics*. 2012;**79**:1015
- [12] Fahmy MA. Transient magneto-thermo-elastic stresses in an anisotropic viscoelastic solid with and without a moving heat source. *Numerical Heat Transfer, Part A: Applications*. 2012;**61**: 633-650
- [13] Jabbari M, Sohrabpour S, Elsami MR. Mechanical and thermal stresses in a functionally graded hollow cylinder due to radially symmetric loads. *International Journal of Pressure Vessels and Piping*. 2002;**79**:493-497
- [14] Bhandari M, Ashirvad KP. Comparison of functionally graded material plate with metal and ceramic plate under transverse load for various boundary conditions. In: *International Journal of Computer Applications, National Conference in Advances in Technology & Applied Sciences (NCATAS-2014)*; September 2014. pp. 25-29
- [15] Sburlati R, Bardella L. Three-dimensional elastic solutions for functionally graded circular plates. *European Journal of Mechanics - A/Solids*. 2011;**30**:219-235
- [16] Li XY, Li PD, Kang GZ, Pan DZ. Axisymmetric thermo-elasticity field in a functionally graded circular plate of

transversely isotropic material.  
*Mathematics and Mechanics of Solids*.  
2012;**18**:464-475

[17] Fahmy MA. A 2-D DRBEM for generalized magneto-thermo-viscoelastic transient response of rotating functionally graded anisotropic thick strip. *International Journal of Engineering and Technology Innovation*. 2013;**3**:70-85

[18] Fahmy MA. The DRBEM solution of the generalized magneto-thermo-viscoelastic problems in 3D anisotropic functionally graded solids. In: *Proceedings of the 5th International Conference on Coupled Problems in Science and Engineering (Coupled Problems 2013)*; 17–19 June 2013; Ibiza, Spain. pp. 862-872

[19] Fahmy MA, Salem AM, Metwally MS, Rashid MM. Computer implementation of the DRBEM for studying the generalized Thermoelastic responses of functionally graded anisotropic rotating plates with one relaxation time. *International Journal of Applied Science and Technology*. 2013;**3**:130-140

[20] Fahmy MA, Salem AM, Metwally MS, Rashid MM. Computer implementation of the DRBEM for studying the classical uncoupled theory of thermoelasticity of functionally graded anisotropic rotating plates. *International Journal of Engineering Research and Applications*. 2013;**3**: 1146-1154

[21] Fahmy MA, Salem AM, Metwally MS, Rashid MM. Computer implementation of the Drbem for studying the classical coupled thermoelastic responses of functionally graded anisotropic plates. *Physical Science International Journal*. 2014;**4**: 674-685

[22] Fahmy MA. Numerical modeling of coupled Thermoelasticity with

relaxation times in rotating FGAPs subjected to a moving heat source. *Physical Science International Journal*. 2016;**9**:1-13

[23] Fahmy MA. DRBEM sensitivity analysis and shape optimization of rotating magneto-thermo-viscoelastic FGA structures using Golden-section search algorithm based on uniform Bicubic B-splines. *Journal of Advances in Mathematics and Computer Science*. 2017;**25**:1-20

[24] Fahmy MA. A predictor-corrector time-stepping Drbem for shape design sensitivity and optimization of multilayer FGA structures. *Transylvanian Review*. 2017;**XXV**: 5369-5382

[25] Mojdehi AR, Darvizeh A, Basti A, Rajabi H. Three dimensional static and dynamic analysis of thick functionally graded plates by the meshless local Petrov-Galerkin (MLPG) method. *Engineering Analysis with Boundary Elements*. 2011;**35**: 1168-1180

[26] Rekik M, El-Borgi S, Ounaies Z. An embedded mixed-mode crack in a functionally graded magneto-electroelastic infinite medium. *International Journal of Solids and Structures*. 2012;**49**:835-845

[27] Reddy J. Analysis of functionally graded plates. *International Journal for Numerical Methods in Engineering*. 2000;**47**:663-684

[28] Zhong Z, Shang E. Three-dimensional exact analysis of a simply supported functionally gradient piezoelectric plate. *International Journal of Solids and Structures*. 2003;**40**: 5335-5352

[29] Ramirez F, Heyliger PR, Pan E. Static analysis of functionally graded elastic anisotropic plates using a discrete

layer approach. *Composites Part B: Engineering*. 2006;**37**:10-20

[30] Li X, Ding H, Chen W.

Axisymmetric elasticity solutions for a uniformly loaded annular plate of transversely isotropic functionally graded materials. *Acta Mechanica*. 2008;**196**:139-159

[31] Kashtalyan M, Menshykova M. Three-dimensional elasticity solution for sandwich panels with a functionally graded core. *Composite Structures*. 2009;**87**:36-43

[32] Yang B, Ding H, Chen W. Elasticity solutions for a uniformly loaded rectangular plate of functionally graded materials with two opposite edges simply supported. *Acta Mechanica*. 2009;**207**:245-258

[33] Vel SS, Batra RC. Three-dimensional analysis of transient thermal stresses in functionally graded plates. *International Journal of Solids and Structures*. 2003; **40**:7181-7196

[34] Zhang XZ, Kitipornchai S, Liew KM, Lim CW, Peng LX. Thermal stresses around a circular hole in a functionally graded plate. *Journal of Thermal Stresses*. 2003;**26**: 379-390

[35] Ohmichi M, Noda N. Plane thermoelastic problem in a functionally graded plate with an oblique boundary to the functional graded direction. *Journal of Thermal Stresses*. 2007;**30**: 779-799

[36] Ootao Y, Tanigawa Y. Transient thermoelastic analysis for a laminated composite strip with an interlayer of functionally graded material. *Journal of Thermal Stresses*. 2009;**32**:1181-1197

[37] Obata Y, Noda N. Transient thermal stresses in a plate of functionally gradient material. In: Holt JB et al., editors. *Ceramic Trans. Functionally*

*Gradient Materials*. Vol. 34. Westerville, Ohio, USA: The American Ceramic Society; 1993. pp. 403-410

[38] Tanigawa Y, Morishita H, Ogaki S. Derivation of systems of fundamental equations for a three-dimensional thermoelastic field with nonhomogeneous material properties and its application to a semi-infinite body. *Journal of Thermal Stresses*. 1999; **22**:689-711

[39] Cheng ZQ, Batra R. Three-dimensional thermoelastic deformations of a functionally graded elliptic plate. *Composites Part B: Engineering*. 2000; **31**:97-106

[40] Reddy J, Cheng ZQ. Three-dimensional thermomechanical deformations of functionally graded rectangular plates. *European Journal of Mechanics—A/Solids*. 2001;**20**:841-855

[41] Sankar BV, Tzeng JT. Thermal stresses in functionally graded beams. *AIAA Journal*. 2002;**40**:1228-1243

[42] Ootao Y, Tanigawa Y. Three-dimensional solution for transient thermal stresses of an orthotropic functionally graded rectangular plate. *Composite Structures*. 2007;**80**: 10-20

[43] Jabbari M, Dehbani H, Eslami M. An exact solution for classic coupled thermoelasticity in spherical coordinates. *Journal of Pressure Vessel Technology*. 2010;**132**:031201

[44] Jabbari M, Dehbani H, Eslami M. An exact solution for classic coupled thermoelasticity in cylindrical coordinates. *Journal of Pressure Vessel Technology*. 2011;**133**:051204

[45] Akbarzadeh A, Abbasi M, Eslami M. Coupled thermoelasticity of functionally graded plates based on the third-order shear deformation theory. *Thin-Walled Structures*. 2012;**53**:141-155

- [46] Fahmy MA. A three-dimensional generalized magneto-thermo-viscoelastic problem of a rotating functionally graded anisotropic solids with and without energy dissipation. *Numerical Heat Transfer, Part A: Applications*. 2013;**63**:713-733
- [47] Fahmy MA. A 2D time domain DRBEM computer model for magneto-thermoelastic coupled wave propagation problems. *International Journal of Engineering and Technology Innovation*. 2014;**4**:138-151
- [48] Fahmy MA, Salem AM, Metwally MS, Rashid MM. Computer implementation of the DRBEM for studying the generalized thermo elastic responses of functionally graded anisotropic rotating plates with two relaxation times. *British Journal of Mathematics & Computer Science*. 2014;**4**:1010-1026
- [49] Fahmy MA, Al-Harbi SM, Al-Harbi BH. Implicit time-stepping DRBEM for design sensitivity analysis of magneto-thermo- elastic FGA structure under initial stress. *American Journal of Mathematical and Computational Sciences*. 2017;**2**:55-62
- [50] Mazarei Z, Nejad MZ, Hadi A. Thermo-Elasto-plastic analysis of thick-walled spherical pressure vessels made of functionally graded materials. *International Journal of Applied Mechanics*. 2016;**8**:1650054
- [51] Su Z, Jin G, Wang L, Wang D. Thermo-mechanical vibration analysis of size-dependent functionally graded micro-beams with general boundary conditions. *International Journal of Applied Mechanics*. 2018;**10**:1850088
- [52] Tomar SS, Talha M. Thermo-mechanical buckling analysis of functionally graded skew laminated plates with initial geometric imperfections. *International Journal of Applied Mechanics*. 2018;**10**:1850014
- [53] Ueda S, Okada M, Nakaue Y. Transient thermal response of a functionally graded piezoelectric laminate with a crack normal to the bimaterial interface. *Journal of Functionally Graded Materials*. 2017;**31**:14-23
- [54] Valizadeh N, Natarajan S, Gonzalez-Estrada OA, Rabczuk T, Bui T, Bordas SPA. NURBS-based finite element analysis of functionally graded plates: Static bending, vibration, buckling and flutter. *Composite Structures*. 2013;**99**:309-326
- [55] Bhardwaj G, Singh IV, Mishra BK, Bui TQ. Numerical simulation of functionally graded cracked plates using NURBS based XIGA under different loads and boundary conditions. *Composite Structures*. 2015;**126**:347-359
- [56] Sladek J, Sladek V, Zhang C. A local BIEM for analysis of transient heat conduction with nonlinear source terms in FGMs. *Engineering Analysis with Boundary Elements*. 2004;**28**:1-11
- [57] Sladek J, Sladek V, Zhang C. Transient heat conduction analysis in functionally graded materials by the meshless local boundary integral equation method. *Computational Materials Science*. 2003;**28**:494-504
- [58] Sladek J, Sladek V, Krivacek J, Zhang C. Local BIEM for transient heat conduction analysis in 3-D axisymmetric functionally graded solids. *Computational Mechanics*. 2003;**32**:169-176
- [59] Gao XW, Zhang C, Sladek J, Sladek V. Fracture analysis of functionally graded materials by a BEM. *Composites Science and Technology*. 2008;**68**:1209-1215
- [60] Fahmy MA. Implicit-explicit time integration DRBEM for generalized magneto-thermoelasticity problems of rotating anisotropic viscoelastic

functionally graded solids. *Engineering Analysis with Boundary Elements*. 2013; **37**:107-115

[61] Fahmy MA. Generalized magneto-thermo-viscoelastic problems of rotating functionally graded anisotropic plates by the dual reciprocity boundary element method. *Journal of Thermal Stresses*. 2013; **36**: 1-20

[62] Fahmy MA. A computerized DRBEM model for generalized magneto-thermo-visco-elastic stress waves in functionally graded anisotropic thin film/substrate structures. *Latin American Journal of Solids and Structures*. 2014; **11**: 386-409

[63] Fahmy MA. Boundary element solution of 2D coupled problem in anisotropic piezoelectric FGM plates. In: *Proceedings of the 6th International Conference on Computational Methods for Coupled Problems in Science and Engineering (Coupled Problems 2015)*; 18–20 May 2015; Venice, Italy; pp. 382-391

[64] Fahmy MA. 3D DRBEM modeling for rotating initially stressed anisotropic functionally graded piezoelectric plates. In: *Proceedings of the 7th European Congress on Computational Methods in Applied Sciences and Engineering (ECCOMAS 2016)*; 5–10 June 2016; Crete Island, Greece. pp. 7640-7658

[65] Fahmy MA. The effect of anisotropy on the structure optimization using Golden-section search algorithm based on BEM. *Journal of Advances in Mathematics and Computer Science*. 2017; **25**:1-18

[66] Fahmy MA. A time-stepping DRBEM for 3D anisotropic functionally graded piezoelectric structures under the influence of gravitational waves. In: *Proceedings of the 1st GeoMEast International Congress and Exhibition*

(GeoMEast 2017); 15–19 July 2017; Sharm El Sheikh, Egypt. *Facing the Challenges in Structural Engineering, Sustainable Civil Infrastructures*. 2017. pp. 350-365

[67] Fahmy MA. Shape design sensitivity and optimization for two-temperature generalized magneto-thermoelastic problems using time-domain DRBEM. *Journal of Thermal Stresses*. 2018; **41**: 119-138

[68] Fahmy MA. Shape design sensitivity and optimization of anisotropic functionally graded smart structures using bicubic B-splines DRBEM. *Engineering Analysis with Boundary Elements*. 2018; **87**:27-35

[69] Fahmy MA. Modeling and optimization of anisotropic viscoelastic porous structures using CQBEM and moving asymptotes algorithm. *Arabian Journal for Science and Engineering*. 2019; **44**:1671-1684

[70] Fahmy MA. Boundary element algorithm for modeling and simulation of dual phase lag bioheat transfer and biomechanics of anisotropic soft tissues. *International Journal of Applied Mechanics*. 2018; **10**:1850108

[71] Fahmy MA. A new computerized boundary element algorithm for cancer modeling of cardiac anisotropy on the ECG simulation. *Asian Journal of Research in Computer Science*. 2018; **2**: 1-10

[72] Fahmy MA. Boundary element modeling and simulation of Biothermomechanical behavior in anisotropic laser-induced tissue hyperthermia. *Engineering Analysis with Boundary Elements*. 2019; **101**: 156-164

[73] Fahmy MA. Computerized Boundary Element Solutions for Thermoelastic Problems: Applications to Functionally Graded Anisotropic

Structures. Saarbrücken: LAP Lambert Academic Publishing; 2017

[74] Fahmy MA. Boundary Element Computation of Shape Sensitivity and Optimization: Applications to Functionally Graded Anisotropic Structures. Saarbrücken: LAP Lambert Academic Publishing; 2017

[75] Cattaneo C. Sur une forme de l'équation de la chaleur éliminant le paradoxe d'une propagation instantanée. Comptes Rendus de l'Académie des Sciences. 1958;**247**:431-433

[76] Wrobel LC. The Boundary Element Method, Applications in Thermofluids and Acoustics. New York: Wiley; 2002

[77] Guiggiani M, Gigante A. A general algorithm for multidimensional Cauchy principal value integrals in the boundary element method. ASME Journal of Applied Mechanics. 1990;**57**:906-915

[78] Mantič V. A new formula for the C-matrix in the Somigliana identity. Journal of Elasticity. 1993;**33**:191-201

[79] Golub GH, Van Loan CF. Matrix Computations. Oxford: North Oxford Academic; 1983

[80] Bathe KJ. Finite Element Procedures. Englewood Cliffs: Prentice-Hall; 1996

[81] Pazera E, Jędrzyński J. Effect of microstructure in thermoelasticity problems of functionally graded laminates. Composite Structures. 2018; **202**:296-303

[82] Xiong QL, Tian XG. Generalized magneto-thermo-microstretch response during thermal shock. Latin American Journal of Solids and Structures. 2015; **12**:2562-2580